

# New heterometallic coordination polymers constructed from 3d–3d' binuclear nodes†‡§

Diana G. Branzea,<sup>a</sup> Augustin M. Madalan,<sup>a</sup> Samuele Ciattini,<sup>b</sup> Narcis Avarvari,<sup>c</sup> Andrea Caneschi<sup>b</sup> and Marius Andruh<sup>\*a</sup>

Received (in Montpellier, France) 31st March 2010, Accepted 7th June 2010

DOI: 10.1039/c0nj00238k

Heterobinuclear  $[\text{Cu}^{\text{II}}\text{Mn}^{\text{II}}]$  and  $[\text{Cu}^{\text{II}}\text{Co}^{\text{II}}]$  cationic complexes can efficiently act as nodes for designing coordination polymers. The crystal structures of two binuclear precursors,  $[\text{LCuCo}(\text{NO}_3)_2]$  (**1**) and  $[\text{LCuMn}(\text{NO}_3)_2]$  (**2**), have been solved ( $\text{L}^{2-}$  is the dianion of the Schiff base resulting from the 2 : 1 condensation of 3-methoxysalicylaldehyde with 1,3-propanediamine). The nitrate ligands, coordinated to  $\text{Co}^{\text{II}}$  and, respectively, the  $\text{Mn}^{\text{II}}$  ions from the precursors, are easily replaced by *exo*-dentate ligands, resulting in 1-D coordination polymers:  $^1_\infty[\text{L}(\text{H}_2\text{O})\text{CuCo}(\text{oxy-bbz})]\cdot\text{CH}_3\text{CN}\cdot\text{C}_2\text{H}_5\text{OH}$  (**3**),  $^1_\infty[\text{L}(\text{H}_2\text{O})\text{CuCo}(2,5\text{-dhtp})]\cdot\text{CH}_3\text{CN}$  (**5**) and  $^1_\infty[\text{L}(\text{H}_2\text{O})\text{CuMn}(\text{ox})]\cdot 3\text{H}_2\text{O}$  (**6**) ( $\text{oxy-bbz}^{2-}$  = the dianion of 4,4'-oxy-bis(benzoic acid);  $2,5\text{-dhtp}^{2-}$  = the dianion of 2,5-dihydroxy-terephthalic acid;  $\text{ox}^{2-}$  = the dianion of the oxalic acid). In the case of the  $[\text{CuMn}]$  node, the interaction with  $\text{oxy-bbz}^{2-}$  affords a binuclear complex,  $[\text{LCuMn}(\text{oxy-bbz})(\text{H}_2\text{O})_2]$  (**4**).

## Introduction

Almost twenty years ago, Robson formulated and illustrated one of the most powerful synthetic strategies in designing coordination polymers: the node-and-spacer approach.<sup>1</sup> The clever choice of the metal ions, according to their stereochemical preference, and the possibility to synthesize a large variety of *exo*-dentate (divergent) organic ligands (rigid or flexible, bi- or polydentate, symmetric or dissymmetric) afforded a plethora of coordination polymers with various dimensionalities and topologies.<sup>2</sup> The peculiarity of the crystal engineering of hybrid inorganic–organic frameworks arises from the use of metal ions that exert a double function: a structural one (directing and sustaining the network topology) and a functional one (carrying the magnetic, optical, redox or catalytic properties). The architecture of the crystals results from a subtle interplay of organizing forces, the leading role being played by the strong directionality of the metal–ligand coordination bonds. Other non-covalent forces involved in sustaining the supramolecular solid-state architectures are

hydrogen bonds,  $\pi$ – $\pi$  and  $d^{10}$ – $d^{10}$  (aurophilic/argentophilic) interactions.<sup>3</sup>

Most of the reported coordination polymers are constructed from monometallic nodes. Recently, we and others have shown that oligonuclear complexes can also act as nodes.<sup>4</sup> The metal ions interact with the divergent ligand through their easily accessible coordination sites. The presence of two or more metal ions, either identical or different, confers to the node a higher geometrical flexibility. Moreover, the metal–metal intra- and inter-node interactions can lead to new properties. Taking the case of binuclear nodes, both metal ions or only one of them can be involved in the interaction with the spacers (Scheme 1). When the two metal ions differ drastically in their chemical behaviour (one hard and the other one a soft acid), then various coordination polymers can result from the selective interaction of the metal ions with the spacers.<sup>4c</sup> This is valid especially for  $[\text{3d}–\text{4f}]$  nodes.<sup>5</sup> We have obtained such nodes by employing dissymmetric compartmental ligands (Scheme 2). This family of ligands was successfully designed by Costes in order to obtain binuclear  $3\text{d}–\text{4f}$  complexes.<sup>6</sup> Recently, we and others observed that these ligands are able to accommodate different 3d metal ions as well.<sup>7</sup> Herein, we report on new heterobimetallic coordination polymers that are obtained by using such  $3\text{d}–\text{3d}'$  nodes and dicarboxylate spacers: the dianion of the 4,4'-oxy-bis(benzoic acid) ( $\text{oxy-bbz}^{2-}$ ), the dianion of the 2,5-dihydroxy-terephthalic acid ( $2,5\text{-dhtp}^{2-}$ ) and the oxalato ligand ( $\text{ox}^{2-}$ ).

## Results and discussion

Three new coordination polymers ( $^1_\infty[\text{L}(\text{H}_2\text{O})\text{CuCo}(\text{oxy-bbz})]\cdot\text{CH}_3\text{CN}\cdot\text{C}_2\text{H}_5\text{OH}$ ,  $^1_\infty[\text{L}(\text{H}_2\text{O})\text{CuCo}(2,5\text{-dhtp})]\cdot\text{CH}_3\text{CN}$  and  $^1_\infty[\text{L}(\text{H}_2\text{O})\text{CuMn}(\text{ox})]\cdot 3\text{H}_2\text{O}$ ) have been constructed from the following heterometallic nodes:  $[\text{LCuMn}]^{2+}$  and  $[\text{LCuCo}]^{2+}$  ( $\text{L}^{2-}$  is the dianion of the Schiff base resulted from the 2 : 1 condensation of 3-methoxysalicylaldehyde with

<sup>a</sup> University of Bucharest, Faculty of Chemistry, Inorganic Chemistry Laboratory, Str. Dumbrova Rosie nr. 23, 020464-Bucharest, Romania. E-mail: marius.andruh@dnt.ro

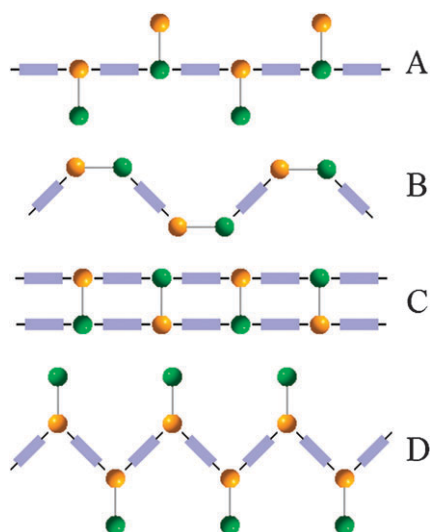
<sup>b</sup> Laboratory of Molecular Magnetism, Dipartimento di Chimica e UdR INSTM di Firenze, Università degli Studi di Firenze, Polo Scientifico, Via della Lastruccia 3, 50019 Sesto Fiorentino, Firenze, Italy

<sup>c</sup> Laboratoire Chimie et Ingénierie Moléculaire (CIMA), UMR 6200 CNRS-Université d'Angers, UFR Sciences, Bât. K, 2 Bd. Lavoisier, 49045 Angers, France

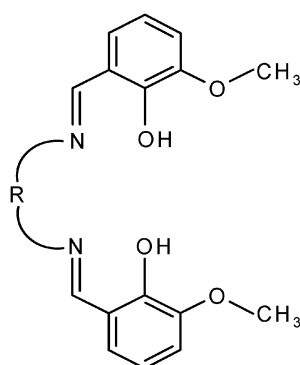
† Dedicated to Professor Herbert W. Roesky, on the occasion of his 75th birthday.

‡ This article is part of a themed issue on Coordination polymers: structure and function.

§ Electronic supplementary information (ESI) available: Further experimental data. CCDC reference numbers 772170–772175. For ESI and crystallographic data in CIF or other electronic format see DOI: 10.1039/c0nj00238k



Scheme 1



Scheme 2

1,3-propanediamine). Binuclear nodes are formed through the interaction of the mononuclear precursor [LCu] with the second metal ion in the presence of the organic spacer.

The *in situ* formation of heterobinuclear nodes prompted us to check whether it is possible to synthesize and isolate the binuclear complexes themselves. The reaction between the mononuclear copper(II) complex [LCu], cobalt(II) nitrate and, respectively, manganese(II) nitrate, affords, after slow evaporation of the solvents, single crystals of compounds [LCuCo(NO<sub>3</sub>)<sub>2</sub>] (**1**) and [LCuMn(NO<sub>3</sub>)<sub>2</sub>] (**2**), which are isomorphous. The crystal structure of compound **1** is depicted in Fig. 1. In both binuclear complexes, the copper(II) ion is hosted into the N<sub>2</sub>O<sub>2</sub> compartment, displaying a square-planar geometry. The cobalt(II) and manganese(II) ions in **1** and, respectively, **2** are hosted into the outer O<sub>2</sub>O'<sub>2</sub> compartment of the ligand. Both are heptacoordinated by four oxygen atoms arising from the organic ligand, and by three oxygen atoms from one chelating and one monodentate nitrate group. In compound **1**, the Co–O distances vary between 2.038(3) and 2.405(3) Å, with long Co–O(methoxy) bonds. The Mn–O distances in crystal **2** vary between 2.1830(18) and 2.384(2) Å. The two long distances correspond to Mn–O(methoxy) bonds. The distances between the metal ions in **1** and **2** are, respectively: Cu···Co = 3.1982(8) and Cu···Mn = 3.3219(6) Å. Selected bond distances are collected in Table 1.

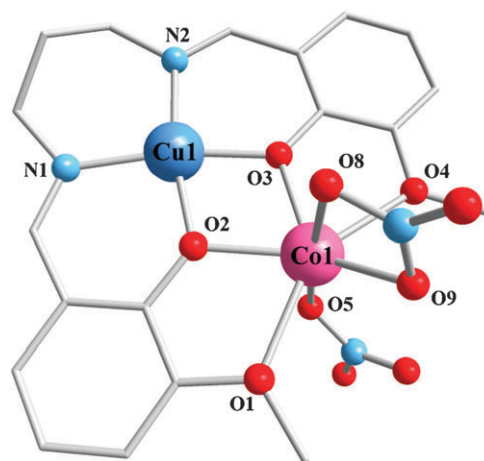


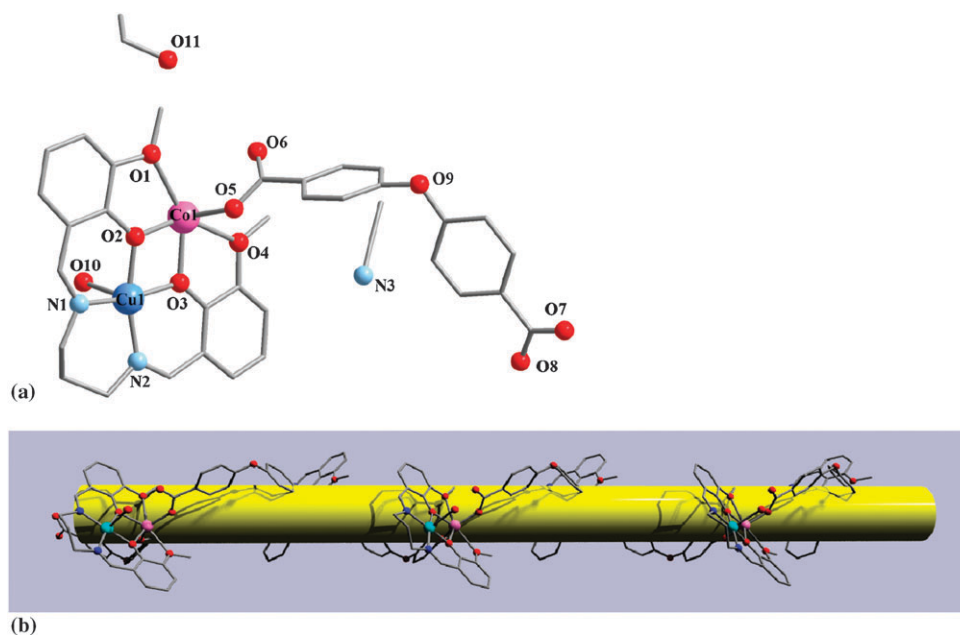
Fig. 1 Molecular structure for the binuclear precursor: [LCuCo(NO<sub>3</sub>)<sub>2</sub>] **1**.

In order to obtain new coordination polymers based on the nodes [CuCo] and [CuMn], we followed the same general synthetic procedure, which consists of the slow diffusion of the [LCuM(NO<sub>3</sub>)<sub>2</sub>] or [LCuM(ClO<sub>4</sub>)<sub>2</sub>] precursor, generated *in situ* through the reaction between the mononuclear copper(II) complex and the nitrate or the perchlorate of the second metal ion (Co<sup>II</sup>, Mn<sup>II</sup>), into a solution of the corresponding polycarboxylic acid fully deprotonated by lithium hydroxide.

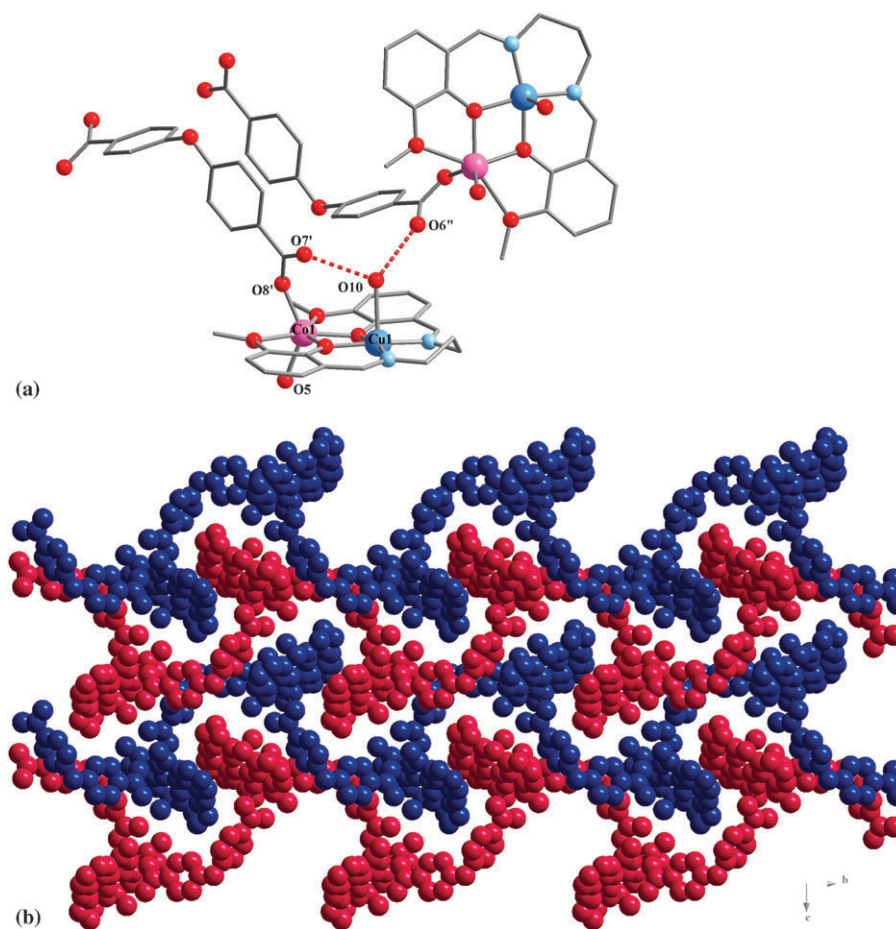
Let us start with the crystal structure of the coordination polymer constructed from the [LCuCo] node and the dianion of the 4,4'-oxy-bis(benzoic acid) (oxy-bbz<sup>2-</sup>) as a spacer: <sup>1</sup><sub>∞</sub>[L(H<sub>2</sub>O)CuCo(oxy-bbz)]·CH<sub>3</sub>CN·C<sub>2</sub>H<sub>5</sub>OH **3**. Within the {CuCo} heterobinuclear unit, the copper(II) ion occupies the inner N<sub>2</sub>O<sub>2</sub> compartment of the Schiff base ligand, while the cobalt(II) ion is hosted into the external O<sub>2</sub>O'<sub>2</sub> compartment of the same ligand (Fig. 2). The copper(II) is pentacoordinated within a square-pyramidal geometry, the basal plane being formed by the four atoms of the N<sub>2</sub>O<sub>2</sub> compartment (Fig. 2a). The apical position is occupied by one aqua ligand [Cu1–O10 = 2.306(3) Å]. There are six oxygen atoms surrounding the cobalt(II) ion (Fig. 2a): four atoms from the O<sub>2</sub>O'<sub>2</sub> compartment of the Schiff base ligand [two short Co1–O bonds, Co1–O2 = 2.022(3), Co1–O3 = 2.025(3) Å, involving the O(phenoxo) atoms and two long bonds involving the methoxy groups: Co1–O1 = 2.407(3) and Co1–O4 = 2.461(3) Å] and two other oxygen atoms from carboxylato groups

Table 1 Selected bond distances for compounds **1** and **2**

Compound	<b>1</b>	<b>2</b>
Bond length/Å		
	Co1–O1 = 2.367(3)	Mn1–O1 = 2.369(2)
	Co1–O2 = 2.063(2)	Mn1–O2 = 2.1830(18)
	Co1–O3 = 2.089(3)	Mn1–O3 = 2.185(2)
	Co1–O4 = 2.405(3)	Mn1–O4 = 2.384(2)
	Co1–O5 = 2.038(3)	Mn1–O5 = 2.192(3)
	Co1–O8 = 2.257(3)	Mn1–O8 = 2.343(3)
	Co1–O9 = 2.094(3)	Mn1–O9 = 2.267(3)
	Cu1–O2 = 1.935(2)	Cu1–O2 = 1.9315(18)
	Cu1–O3 = 1.926(3)	Cu1–O3 = 1.9317(19)
	Cu1–N1 = 1.969(3)	Cu1–N1 = 1.969(2)
	Cu1–N2 = 1.979(3)	Cu1–N2 = 1.978(2)



**Fig. 2** Crystal structure of  $1_{\infty}[\text{L}(\text{H}_2\text{O})\text{CuCo}(\text{oxy-bbz})]\cdot\text{CH}_3\text{CN}\cdot\text{C}_2\text{H}_5\text{OH}$  (**3**): asymmetric unit and atom numbering scheme (a); view of a helical chain (b); packing diagram showing chains of opposite chiralities.



**Fig. 3** Details of the packing diagram for crystal **3**: intra- and intermolecular hydrogen bonds—symmetry transformations:  $' = 1.5 - x, 0.5 + y, 1.5 - y$ ;  $'' = -0.5 + x, 0.5 - y, -0.5 + z$  (a); supramolecular layers resulting from connecting the chains through hydrogen bonds and  $\pi$ - $\pi$  stacking interactions (b).



[Co1–O5 = 1.982(3) and Co1–O8' = 1.947(3) Å ( $' = 1.5 - x, 0.5 + y, 1.5 - y$ ). The 4,4'-oxybis(benzoato) anion is coordinated to two cobalt(II) ions from different nodes through two oxygen atoms, one from each carboxylato group. One of the uncoordinated oxygen atoms of the 4,4'-oxybis(benzoato) anion, O7, forms an intramolecular hydrogen bond with the water molecule coordinated to copper [O7'...O10 = 2.772(5) Å].

The shape of the spacer is angular, with the value of the C24–O9–C27 angle equal to 117.1(3)°. Previous work on V-shaped dicarboxylates, such as the 4,4'-oxybis(benzoato) anion, have shown that by employing this spacer to link metal ions preferring tetrahedral environments, helical structures are obtained.<sup>8</sup> In compound **3**, taking into account only the short metal–ligand interactions, the stereochemistry of the cobalt ion can be described as being tetrahedral. Consequently, the individual chains in **3** are chiral (Fig. 2b). Since **3** crystallizes in a centrosymmetric space group, the crystal contains chains of opposite helicities. These chains are connected through hydrogen bonds (Fig. 3a) established between the aqua ligand coordinated to a copper ion from one chain and a non-coordinated carboxylato oxygen from another chain [O10...O6'' = 2.757(4) Å;  $'' = -0.5 + x, 0.5 - y, -0.5 + z$ ] resulting in supramolecular layers which are parallel to the *bc* crystallographic plane (Fig. 3b). We recall that the aqua ligand is involved in two hydrogen bonds, one intra- and the other one intermolecular. The stability of supramolecular layers is reinforced by  $\pi$ – $\pi$  stacking interactions established between the aromatic fragments of both valpn<sup>2-</sup> and oxy-bbz<sup>2-</sup> ligands from neighbouring chains.

Interestingly, the interaction of the [CuMn] node with the oxy-bbz<sup>2-</sup> anion leads to a completely different structure: a discrete complex is obtained with only one carboxylato group coordinated to both metal ions from the binuclear node (*syn-syn* bridging mode): [LCuMn(oxy-bbz)(H<sub>2</sub>O)<sub>2</sub>] (**4**) (Fig. 4). The copper ion is characterized by a distorted square-pyramidal geometry, with the four atoms of the inner N<sub>2</sub>O<sub>2</sub> compartment of the Schiff base ligand in the basal plane, and an oxygen atom from the carboxylato group of

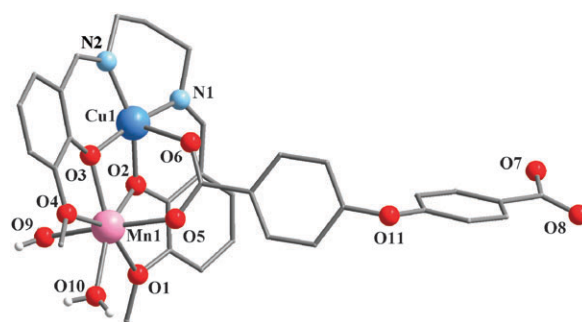


Fig. 4 Crystal structure of compound **4**.

4,4'-oxybis(benzoato) ligand into the apical position. The percentage of trigonal distortion from square-pyramidal geometry is described by the  $\tau$  parameter, defined as  $[(\theta - \varphi)/60] \times 100$ , where  $\theta$  and  $\varphi$  are the angles between the donor atoms forming the plane in a square-pyramidal geometry.<sup>9</sup> The value of the  $\tau$  parameter for the coordination polyhedron of copper(II) in **4** is 0.22 ( $\tau = 0$  for an ideal square-planar geometry and  $\tau = 1$  for an ideal trigonal bipyramidal geometry), indicating a significant distortion from the square-pyramidal geometry. The manganese(II) ion is heptacoordinated and displays a distorted pentagonal bipyramidal geometry. The equatorial plane is formed by five oxygen atoms, four atoms provided by the O<sub>2</sub>O'<sub>2</sub> compartment of the organic ligand and another one from a coordinated water molecule, whereas the axial positions are occupied by oxygen atoms, one from the carboxylato group of the 4,4'-oxybis(benzoato) anion, and the second one from another coordinated water molecule. The Mn–O(methoxy) bonds are quite long: Mn1–O1 = 2.5357(19) and Mn1–O4 = 2.5569(16) Å]. If we neglect them, then a more appropriate description of the manganese environment should be trigonal bipyramidal. The binuclear entities are interconnected through hydrogen bonds established between the water molecules coordinated at the manganese(II) ions and the uncoordinated carboxylate groups belonging to the neighbouring complexes, resulting in a 2D supramolecular architecture (Fig. 5). Each water molecule is involved in hydrogen interactions with

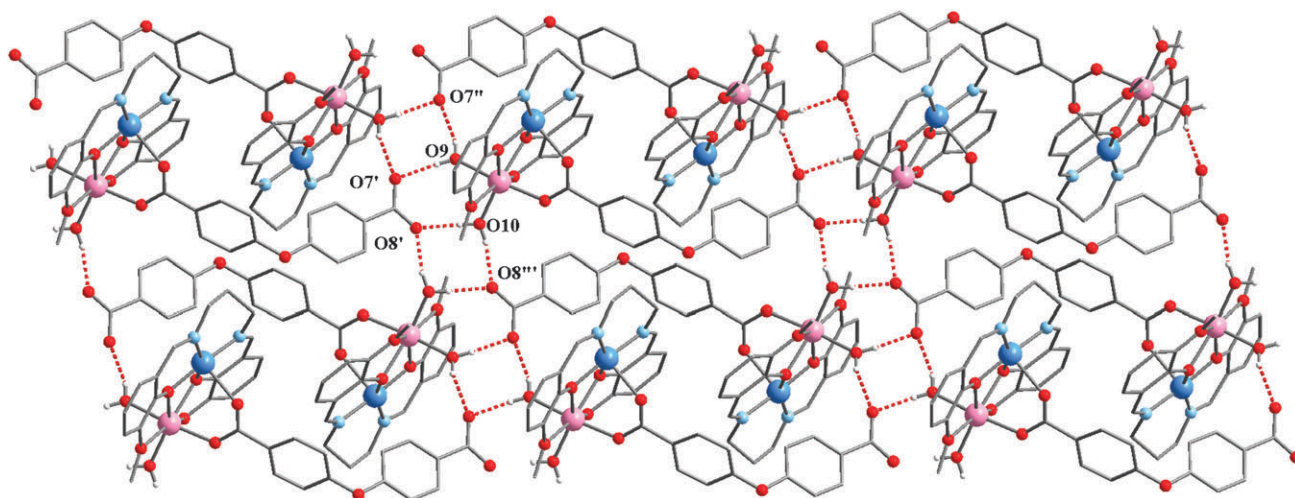


Fig. 5 Packing diagram in crystal **4** showing the supramolecular layers formed by hydrogen bonds (symmetry transformations:  $' = -1 + x, y, 1 + z$ ;  $'' = -x, -y, -z$ ;  $''' = -x, -1 - y, -z$ ).

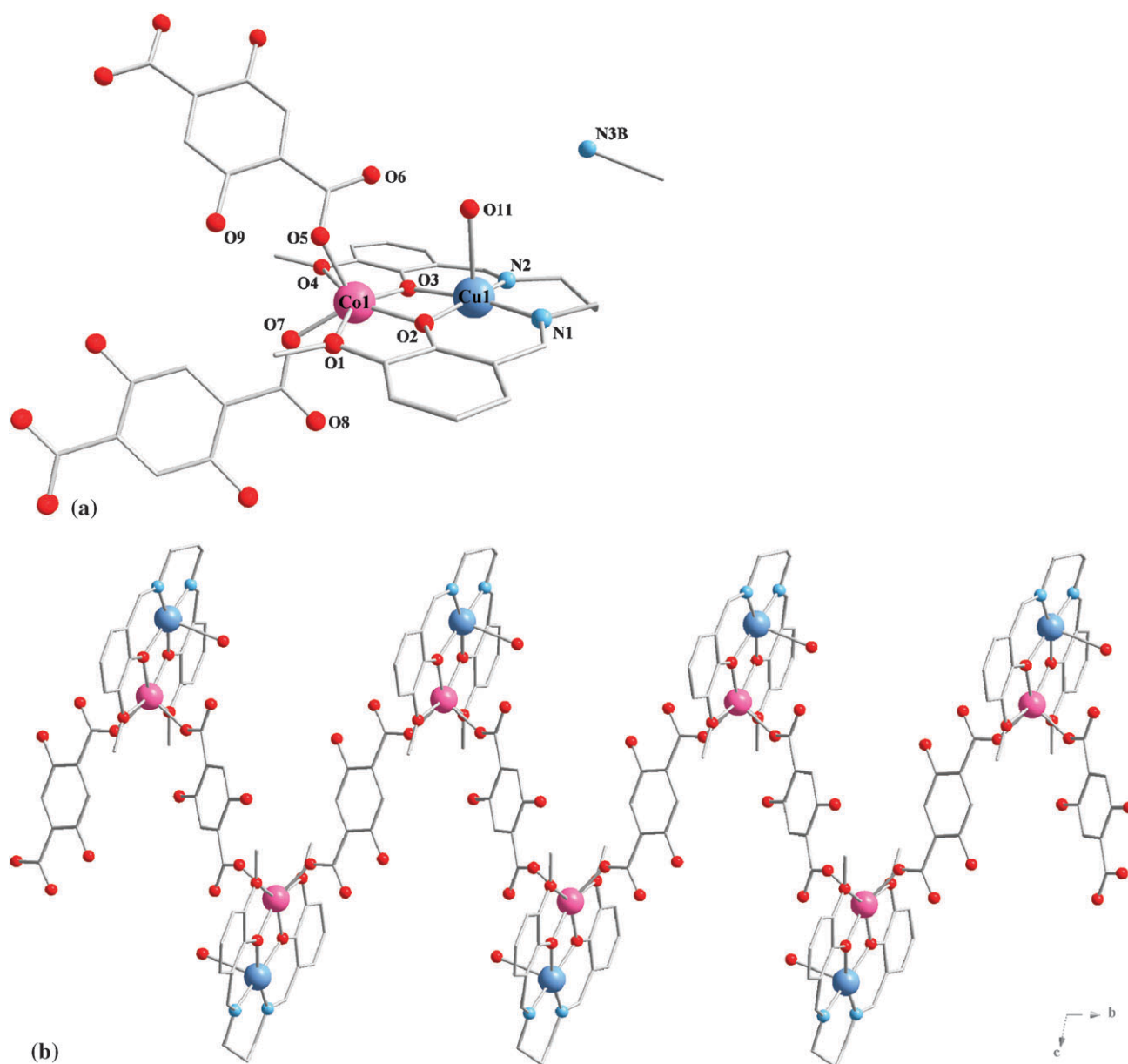


Fig. 6 Crystal structure of compound **5**: asymmetric unit and numbering scheme (a); perspective view of the 1-D coordination polymer (b).

two oxygen atoms from two different carboxylate groups [ $\text{O9}\cdots\text{O7}' = 2.6686(18)$ ,  $\text{O9}\cdots\text{O7}'' = 2.8734(18)$ ,  $\text{O10}\cdots\text{O8}' = 2.6765(18)$ ,  $\text{O10}\cdots\text{O8}''' = 2.6933(19)$  Å;  $' = -1 + x, y, 1 + z$ ;  $'' = -x, -y, -z$ ;  $''' = -x, -1 - y, -z$ ].

The interaction of the  $[\text{LCuCo}]^{2+}$  node with the dianion the 2,5-dihydroxy-terephthalic acid ( $2,5\text{-dhtp}^{2-}$ ) affords a 1-D coordination polymer:  ${}^1_{\infty}[\text{L}(\text{H}_2\text{O})\text{CuCo}(2,5\text{-dhtp})]\cdot\text{CH}_3\text{CN}$  (**5**). The heterobinuclear  $\{\text{CuCo}\}$  nodes are connected by 2,5-dihydroxy-terephthalato anions *via* the cobalt(II) ions generating infinite zigzag chains (Fig. 6). The cobalt(II) ion is hosted into the external  $\text{O}_2\text{O}'_2$  compartment of the organic ligand. The coordination sphere of the Cu(II) ion is formed by the four atoms of the  $\text{N}_2\text{O}_2$  compartment in the basal plane and another oxygen atom from the aqua ligand coordinated in the apical position, and its geometry can be characterized as square-pyramidal. The apical Cu–O bond is

longer [ $\text{Cu2–O11} = 2.4136(24)$  Å] than the other four bonds in the basal plane [ $\text{Cu2–N1} = 1.980(3)$ ;  $\text{Cu2–N2} = 1.975(3)$ ;  $\text{Cu2–O2} = 1.9550(18)$ ;  $\text{Cu2–O3} = 1.9634(18)$  Å]. The coordination sphere of the cobalt ion is formed by four oxygen atoms provided by the  $\text{valpn}^{2-}$  ligand [ $\text{Co1–O1} = 2.4892(21)$ ;  $\text{Co1–O4} = 2.5427(22)$ ;  $\text{Co1–O2} = 2.0047(19)$ ;  $\text{Co1–O3} = 2.0172(18)$  Å] and other two oxygen atoms from the carboxylate groups of two 2,5-dihydroxy-terephthalato anions [ $\text{Co1–O7} = 1.950(2)$  Å;  $\text{Co1–O5} = 1.992(2)$  Å]. As in the other cases of binuclear complexes derived from this ligand, the methoxy groups are weakly bonded to the second 3d metal ion.

Each carboxylate group is coordinated to a cobalt ion through one oxygen atom. The two hydroxo groups of the 2,5-dihydroxy-terephthalato spacer did not increase the dimensionality of the system *via* hydrogen bonds, the only hydrogen bond in which each HO group is involved being an

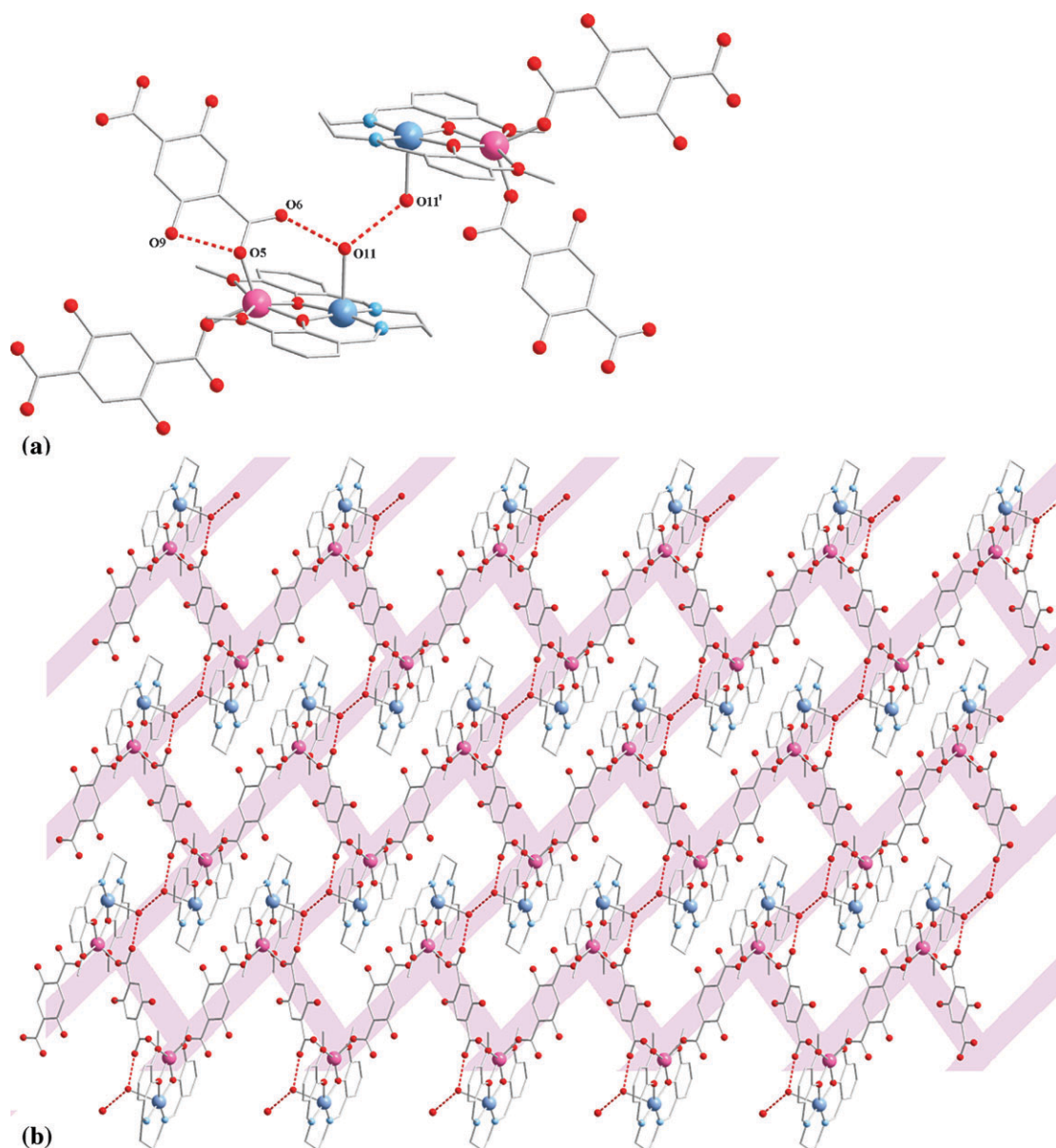


**Fig. 7** Packing diagram in crystal **5**: intra- and intermolecular hydrogen bonds—symmetry transformation:  $' = -1 - x, 2 - y, -z$  (a); perspective view of a brick wall supramolecular layer (b).

intramolecular one [ $O09 \cdots O05 = 2.569(3) \text{ \AA}$ ], where the hydroxy group acts as a donor toward the oxygen atom of the closest carboxylato group, coordinated at the Co(II) ion. Each aqua ligand coordinated to the copper(II) ion forms hydrogen bonds: an intramolecular interaction, with the uncoordinated oxygen atom of the carboxylato group from the nearby spacer [ $O01 \cdots O06 = 2.709(4) \text{ \AA}$ ], and an intermolecular one with the aqua ligand [ $O01 \cdots O01' = 2.876(3) \text{ \AA}; ' = -1 - x, 2 - y, -z$ ] from the neighbouring zig-zag chain (Fig. 7a). A 2-D supramolecular sheet with a (6,3) brick wall topology is developed within the  $bc$  crystallographic plane (Fig. 7b).

A useful tool to diagnose the stereochemistry of the cobalt(II) ion is the UV-vis spectroscopy.<sup>10</sup> The diffuse reflectance spectra of compounds **3** and **5** are a superposition of the absorption bands of the two chromophores (Fig. 8). The

intense band located at  $\sim 600 \text{ nm}$  is characteristic for cobalt(II) complexes with a tetrahedral geometry, being ascribed to the  $^4A_2 \rightarrow ^4T_1(P)$  transition. Another characteristic band for tetrahedral cobalt(II) complexes is located in the near-infrared region, which is assigned to the  $^4A_2 \rightarrow ^4T_1(F)$  transition. When the symmetry of the cobalt(II) ion decreases from  $T_d$  to  $C_{2v}$ , the  $^4T_1(F)$  term is split into  $^4A_2 + ^4B_1 + ^4B_2$  levels and three bands are expected. Indeed, in the NIR region, both compounds show broad bands between 1000 and 2000 nm, each band with three not-well defined maxima. Consequently, the stereochemistry of the cobalt(II) ion in compounds **3** and **5** can be described as being (pseudo)tetrahedral, with a symmetry close to  $C_{2v}$ .

The ability of the oxalato anion to generate homo- and heteropolynuclear complexes with various nuclearities or



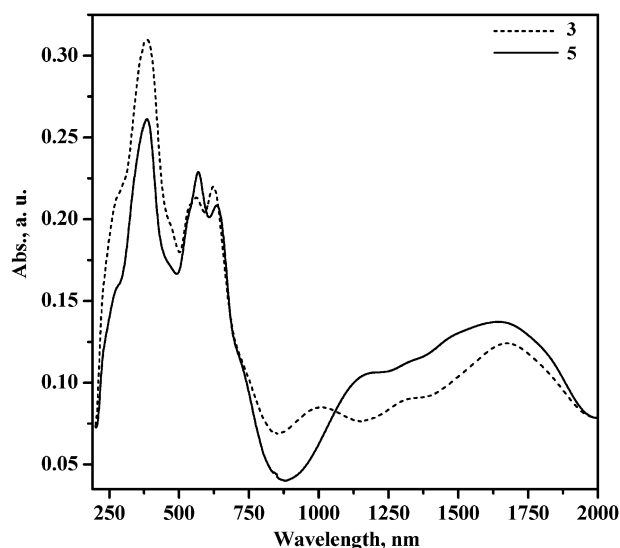


Fig. 8 Diffuse reflectance spectra of compounds 3 and 5.

dimensionalities is well known.<sup>11</sup> There are two common bridging modes exhibited by the oxalato ligand: (i) bis-chelating toward two metal centers; (ii) bidentate chelating toward one metal ion and monodentate toward the second one. The self-assembly process involving  $[\text{LCuMn}]^{2+}$  and  $\text{C}_2\text{O}_4^{2-}$  ions affords an oxalato-bridged coordination polymer:  $\infty[\text{L}(\text{H}_2\text{O})\text{CuMn}(\text{ox})]\cdot 3\text{H}_2\text{O}$  (**6**). The oxalato anion connects the binuclear  $\{\text{CuMn}\}$  nodes through the manganese(II) ions,

generating infinite chains running along the crystallographic  $b$  axis. The oxalato ions exhibit a second bridging mode: chelated to one manganese ion and monodentate to another (Fig. 9a). The copper(II) ion is surrounded by five atoms, four atoms from the  $\text{N}_2\text{O}_2$  compartment of the Schiff base ligand defining the basal plane and one water molecule in the apical position, resulting in a slightly distorted square-pyramidal geometry (Fig. 9b). The value of the  $\tau$  parameter (0.06) indicates an insignificant distortion from the ideal square-pyramidal geometry. The manganese(II) ions are heptacoordinated, the coordination sphere being formed by the four oxygen atoms provided by the  $\text{O}_2\text{O}_2'$  compartment of the organic ligand and other three oxygen atoms from two oxalato anions (Fig. 10a). Again the Mn–O(methoxy) distances, Mn1–O1 = 2.413(2) and Mn1–O4 = 2.424(2) Å, are longer than the other Mn–O distances. The Cu...Mn separation through the bridging phenoxo oxygen atoms of the valpn<sup>2-</sup> ligand is equal to 3.339(1) Å. The distance between the oxalato-bridged manganese ions is 5.858(2) Å.

Apart from the aqua ligand coordinated at the copper(II) ion, there are three other crystallization water molecules per heterobinuclear  $\{\text{CuMn}\}$  unit. The coordinated water molecule is involved in two intramolecular hydrogen bonds with vicinal oxygen atoms provided by two oxalato spacers, one atom uncoordinated ( $\text{O1W}'' \cdots \text{O7}' = 2.78$  Å;  $' = 0.5 - x, 0.5 + y, 0.5 - z; '' = 0.5 - x, -0.5 + y, 0.5 - z$ ) and the other one coordinated to the manganese ion ( $\text{O1W}' \cdots \text{O5} = 2.82$  Å) (Fig. 10a). In the crystallographic  $ab$  plane, the chains

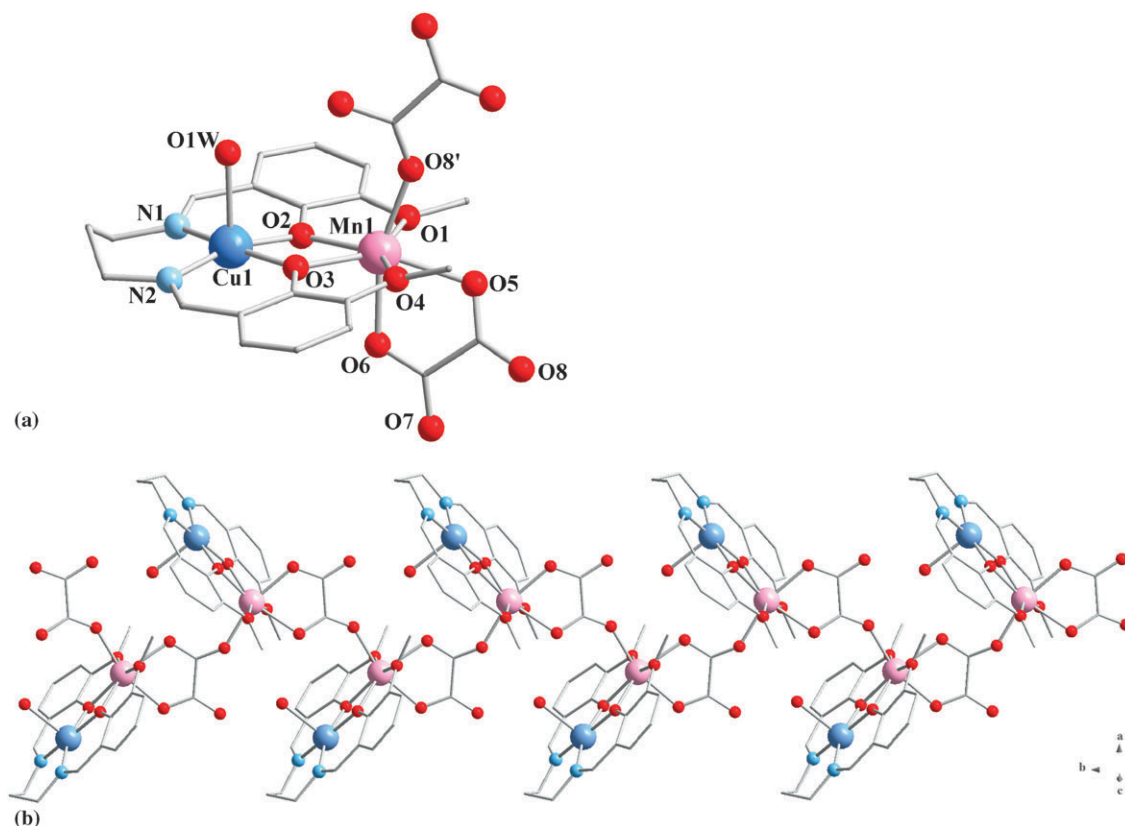
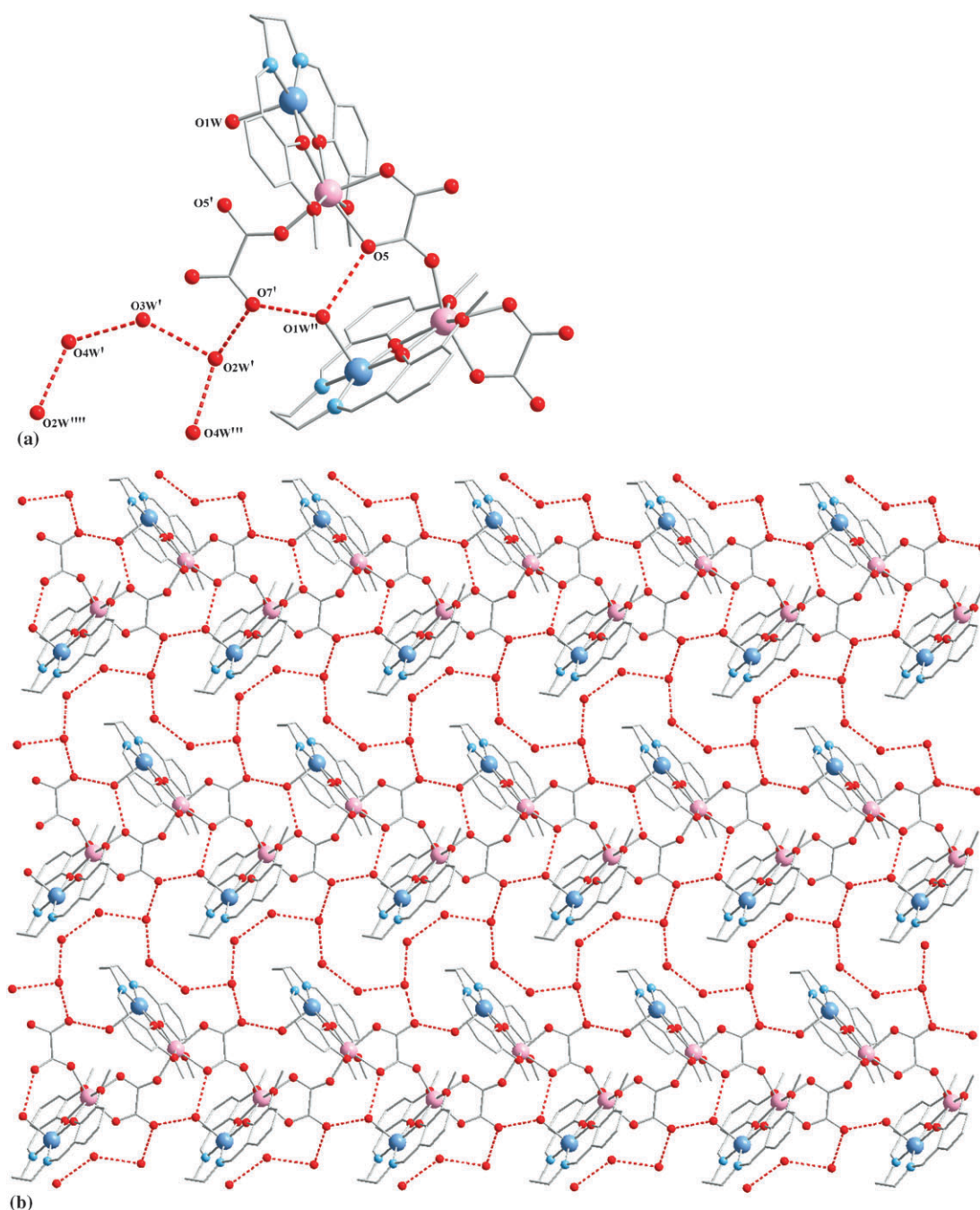


Fig. 9 Crystal structure of **6**: view of the asymmetric unit along with the atom numbering scheme (a)  $' = \frac{1}{2} - x, \frac{1}{2} + y, \frac{1}{2} - z$ ; view of a chain (b).



**Fig. 10** Details of the packing diagram for crystal **6**: hydrogen bonds involving the coordinated and uncoordinated water molecules (a); perspective view of a supramolecular layer (b).

are interconnected into a 2D supramolecular layer through a complex system of hydrogen bonds established between the crystallization water molecules ( $O2W' \cdots O7' = 2.87$ ,  $O2W' \cdots O3W' = 2.84$ ,  $O3W' \cdots O4W' = 2.85$ ,  $O4W' \cdots O2W''' = 2.76$ ,  $O2W' \cdots O4W''' = 2.76$  Å;  $''' = 1 + x, y, z$ ;  $'''' = 1 + x, 1 + y, z$ ) (Fig. 10b). The hydrogen bonded crystallization water molecules form helical chains, which show both *P* and *M* chiralities (Fig. 11). Other chains made by hydrogen bonded water molecules, including helical chains, have been reported recently in the literature.<sup>12</sup> Selected bond distances for compounds **3–6** are given in Table 2.

In a previous paper,<sup>7b</sup> we investigated the magnetic properties of coordination polymers constructed from binuclear [CuMn] nodes connected by dicarboxylato and  $[Ni(CN)_4]^{2-}$  spacers. Since the distance between the nodes is quite large, the interaction between the resulting spins ( $S = 2$ , antiferromagnetic intranode coupling) was found to be extremely weak, according to the Weiss constant we found in these complexes. Complex **6** seems to be more interesting from this point of view because the binuclear nodes are linked by a shorter spacer ( $ox^{2-}$ ). The temperature dependence of the  $\chi_M T$  product ( $\chi_M$  is the magnetic susceptibility per  $Cu^{II}Mn^{II}$  unit) is similar to those



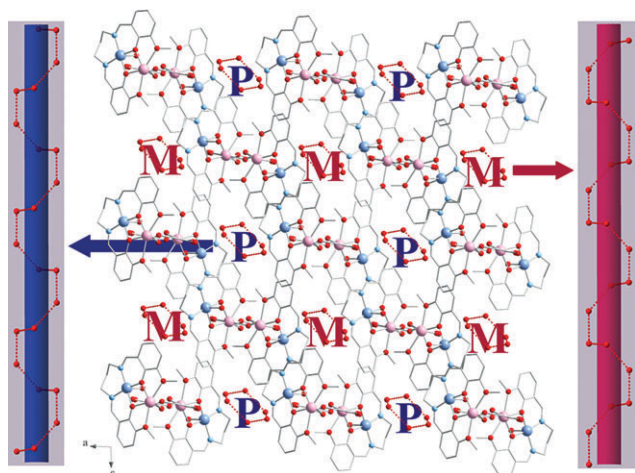


**Fig. 11** Packing diagram in crystal **6** showing the hosted water chains.

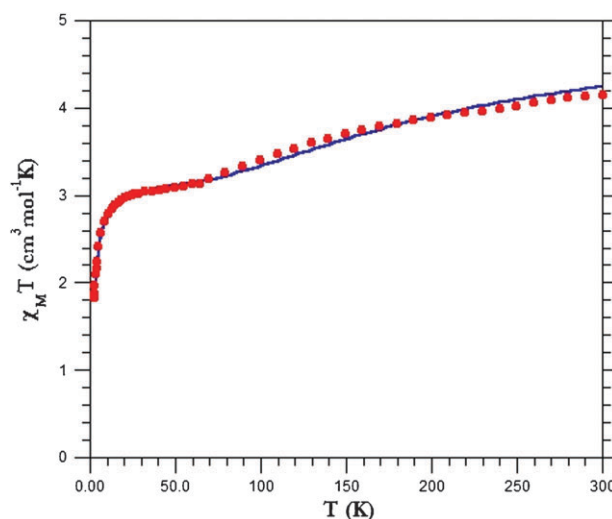


**Fig. 12**  $\chi_M T$  vs.  $T$  curve for compound **6**.

observed with other complexes in this family (Fig. 12). The room temperature value of the  $\chi_M T$  product is  $4.15 \text{ cm}^3 \text{ mol}^{-1} \text{ K}$ , lower than that expected ( $4.75 \text{ cm}^3 \text{ mol}^{-1} \text{ K}$ ) for a  $[\text{CuMn}]$  pair with uncoupled ions (assuming  $g_{\text{Cu}} = g_{\text{Mn}} = 2$ ), suggesting that the intra-node antiferromagnetic interaction is effective even at room temperature. By lowering the temperature,  $\chi_M T$  decreases continuously down to 50 K, reaching a plateau, then it decreases abruptly. This behavior can be interpreted as follows: upon cooling, the  $\text{Cu}^{\text{II}}$  and  $\text{Mn}^{\text{II}}$  ions within each node are antiferromagnetically coupled. Indeed, the observed plateau corresponds to  $S = 2$  ( $3.03 = \text{cm}^3 \text{ mol}^{-1} \text{ K}$ ). The further decrease of the temperature is due to the intrachain antiferromagnetic interactions of the  $S = 2$  spins and, eventually, to the zero-field splitting effect within the  $S = 2$  spin state. For the  $\text{Cu}^{\text{II}} (S = \frac{1}{2})$ – $\text{Mn}^{\text{II}} (S = \frac{5}{2})$  system, the energies of the low-lying spin states are obtained by using the isotropic spin Hamiltonian:  $H = -JS_{\text{Mn}}S_{\text{Cu}}$ , which leads to the following equation describing the temperature dependence of susceptibility,  $\chi_M$ :

$$\chi_M = [2N\beta^2 g^2 / k(T - \theta)] [(5 + 14 \exp(x)) / (5 + 7 \exp(x))];$$

with  $x = 3J/kT$ .

The Weiss term,  $\theta$ , was included in order to take into account the inter-node and other intermolecular interactions. A least-squares fit to the data leads to the following values:  $J = -71.6 \text{ cm}^{-1}$ ;  $g = 2.06$ ;  $\theta = -1.56 \text{ K}$ . The Weiss constant is sensibly higher than the values found for  $[\text{LCuMn}(\text{pzdc})(\text{CH}_3\text{OH})(\text{H}_2\text{O})] \cdot \text{H}_2\text{O}$  ( $\theta = -0.41 \text{ K}$ ) and  $[\text{LCu}(\text{CH}_3\text{OH})(\text{H}_2\text{O})\text{Mn}(\text{NC})_2\text{Ni}(\text{CN})_2] \cdot (\text{H}_2\text{O})(\text{CH}_3\text{CN})$  ( $\theta = -0.39 \text{ K}$ ),<sup>7b</sup> suggesting, as expected, a stronger inter-node antiferromagnetic interaction ( $\text{pzdc}^{2-}$  = the dianion of the pyrazole-3,5-dicarboxylic acid). The strength of the inter-node coupling ( $J' = -0.27 \text{ cm}^{-1}$ ) has been estimated by using the following equation:  $\theta = z \cdot J' \cdot S(S + 1) / 3k$ , where  $z = 2$  ( $z$  is the number of nearest neighbors) and  $S = 2$ . This is valid assuming that the magnetic interaction between the chains is negligible. Alternatively, the data below 50 K have been fitted through the Fisher equation for a classical uniform chain of local spin quintets:<sup>13</sup>

$$\chi_M T = \frac{Ng^2 \beta^2}{3k} S(S + 1) \cdot \left( \frac{1 + u}{1 - u} \right)$$

with  $u = \coth[J'S(S + 1)/kT] - [kT/J'S(S + 1)]$  and  $S = 2$ .

**Table 2** Selected bond distances for compounds **3–6**<sup>a</sup>

Compound	3	4	5	6
Bond length/Å	Co1–O8 = 1.947(3) Co1–O5 = 1.982(3) Co1–O2 = 2.022(3) Co1–O3 = 2.025(3) Co1–O1 = 2.407(3) Co1–O4 = 2.461(3) Cu1–N1 = 1.977(3) Cu1–N2 = 1.981(3) Cu1–O2 = 1.956(3) Cu1–O3 = 1.944(2) Cu1–O10 = 2.306(3)	Mn1–O10 = 2.1230(13) Mn1–O5 = 2.1260(13) Mn1–O3 = 2.1485(13) Mn1–O2 = 2.1946(13) Mn1–O9 = 2.1998(14) Mn1–O1 = 2.5357(19) Mn1–O4 = 2.5569(16) Cu1–N1 = 1.9730(16) Mn1–O9 = 2.0050(18) Cu1–O2 = 1.9755(14) Cu1–O3 = 1.9336(12) Cu1–O6 = 2.2947(14)	Co1–O7 = 1.950(2) Co1–O5 = 1.992(2) Co1–O2 = 2.0047(19) Co1–O3 = 2.0172(18) Co1–O1 = 2.4892(21) Co1–O4 = 2.5427(22) Cu2–N1 = 1.980(3) Cu2–N2 = 1.975(3) Cu2–O2 = 1.9550(18) Cu2–O3 = 1.9634(18) Cu2–O11 = 2.414(3)	Mn1–O1 = 2.413(2) Mn1–O2 = 2.179(2) Mn1–O3 = 2.1994(19) Mn1–O4 = 2.424(2) Mn1–O5 = 2.241(2) Mn1–O6 = 2.165(2) Mn1–O8' = 2.134(2) Cu1–N1 = 1.973(3) Cu1–N2 = 2.000(2) Cu1–O2 = 1.9855(19) Cu1–O3 = 1.931(2) Cu1–O1W = 2.269(2)

<sup>a</sup> Symmetry code: ' = 0.5 – x, 0.5 + y, 0.5 – z.

**Table 3** Crystallographic data, details of data collection and structure refinement parameters for compounds 1–6

Compound	1	2	3
Chemical formula	C <sub>19</sub> H <sub>20</sub> CoCuN <sub>4</sub> O <sub>10</sub>	C <sub>19</sub> H <sub>20</sub> CuMnN <sub>4</sub> O <sub>10</sub>	C <sub>37</sub> H <sub>39</sub> CoCuN <sub>5</sub> O <sub>11</sub>
<i>M</i> /g mol <sup>−1</sup>	586.86	582.87	824.18
Temperature/K	293(2)	293(2)	200(2)
Wavelength/Å	0.71073	0.71073	0.71073
Crystal system	Triclinic	Triclinic	Monoclinic
Space group	<i>P</i> $\bar{1}$	<i>P</i> $\bar{1}$	<i>P</i> 2 <sub>1</sub> / <i>n</i>
<i>a</i> /Å	8.5076(15)	8.6001(10)	10.5871(16)
<i>b</i> /Å	11.190(2)	11.2045(15)	20.8938(11)
<i>c</i> /Å	11.3624(18)	11.3972(13)	16.6956(16)
$\alpha$ (°)	82.947(13)	83.875(10)	90
$\beta$ (°)	83.930(13)	84.626(9)	107.580(10)
$\gamma$ (°)	84.633(14)	84.262(10)	90
<i>V</i> /Å <sup>3</sup>	1063.9(3)	1082.7(2)	3520.7(7)
<i>Z</i>	2	2	4
<i>D</i> <sub>c</sub> /g cm <sup>−3</sup>	1.832	1.788	1.555
$\mu$ /mm <sup>−1</sup>	1.847	1.632	1.143
<i>F</i> (000)	596	592	1704
Goodness-of-fit on <i>F</i> <sup>2</sup>	1.013	1.083	1.036
Final <i>R</i> 1, <i>wR</i> <sub>2</sub> [ <i>I</i> > 2σ( <i>I</i> )]	0.0621, 0.1428	0.0565, 0.1066	0.0538, 0.1320
<i>R</i> <sub>1</sub> , <i>wR</i> <sub>2</sub> (all data)	0.1211, 0.1733	0.0900, 0.1174	0.0977, 0.1560
Largest diff. peak and hole/e Å <sup>−3</sup>	0.699, −0.724	0.373, −0.742	1.081, −0.744

Compound	4	5	6
Chemical formula	C <sub>33</sub> H <sub>32</sub> CuMnN <sub>2</sub> O <sub>11</sub>	C <sub>29</sub> H <sub>29</sub> CoCuN <sub>3</sub> O <sub>11</sub>	C <sub>21</sub> H <sub>28</sub> CuMnN <sub>2</sub> O <sub>12</sub>
<i>M</i> /g mol <sup>−1</sup>	751.09	717.98	618.87
Temperature/K	293(2)	293(2)	293(2)
Wavelength/Å	0.71073	0.71073	0.71073
Crystal system	Triclinic	Triclinic	Monoclinic
Space group	<i>P</i> $\bar{1}$	<i>P</i> $\bar{1}$	<i>P</i> 2 <sub>1</sub> / <i>n</i>
<i>a</i> /Å	9.7256(6)	9.8331(15)	15.236(5)
<i>b</i> /Å	10.3820(6)	11.3315(16)	10.124(5)
<i>c</i> /Å	16.7920(10)	13.8667(19)	15.653(5)
$\alpha$ (°)	73.999(4)	99.618(11)	90
$\beta$ (°)	73.386(5)	96.924(12)	93.066(5)
$\gamma$ (°)	89.498(5)	93.266(12)	90
<i>V</i> /Å <sup>3</sup>	1557.26(16)	1507.6(4)	2411.0(16)
<i>Z</i>	2	2	4
<i>D</i> <sub>c</sub> /g cm <sup>−3</sup>	1.602	1.571	1.683
$\mu$ /mm <sup>−1</sup>	1.155	1.321	1.474
<i>F</i> (000)	772	726	1240
Goodness-of-fit on <i>F</i> <sup>2</sup>	1.026	1.021	1.117
Final <i>R</i> 1, <i>wR</i> <sub>2</sub> [ <i>I</i> > 2σ( <i>I</i> )]	0.0442, 0.0952	0.0594, 0.1316	0.0505, 0.1391
<i>R</i> <sub>1</sub> , <i>wR</i> <sub>2</sub> (all data)	0.0646, 0.1026	0.1067, 0.1529	0.0649, 0.1548
Largest diff. peak and hole/e Å <sup>−3</sup>	0.613, −1.031	0.651, −0.901	1.641, −0.722

The best fit to the data (Fig. S1§) gives  $J' = -0.21 \text{ cm}^{-1}$ , a value that is close to the one obtained from the Weiss constant.

## Conclusions

Herein, we have illustrated with new examples that hetero-bimetallic 3d–3d' nodes can efficiently act as nodes for designing coordination polymers. In principle, the spacers can interact with only one type of metal ion from different nodes, while the second metal ion from the nodes is not involved in the linkage, can connect one type of metal ion from a node with another type from the next node, or can connect both metal ions from a node with the two metal ions from another node (Scheme 1). In the examples we have presented here, only the second metal ion (Co<sup>II</sup>, Mn<sup>II</sup>), which is hosted in the large compartment, interacts with the spacers.

## Experimental section

### Physical measurements

IR spectra were recorded on a Tensor 37 Bruker spectrophotometer in the 4000–400 cm<sup>−1</sup> range. Samples were run as KBr pellets. Diffuse reflectance UV–VIS–NIR spectra have been recorded with a JASCO V670 instrument.

### X-Ray structure determination

X-Ray diffraction measurements were performed on a STOE IPDS II diffractometer for the compounds **1**, **2**, **4** and **5**, on a Nonius Kappa CCD diffractometer for the compound **3** and Oxford Xcalibur 3 CCD diffractometer for the compound **6**, operating with Mo-K $\alpha$  ( $\lambda = 0.71073 \text{ Å}$ ) X-ray tube with graphite monochromator. The structures were solved by direct methods and refined by full-matrix least squares techniques based on  $F^2$ . The non-H atoms were refined with anisotropic

displacement parameters. Calculations were performed using SHELX-97 crystallographic software package. A summary of the crystallographic data and the structure refinement for crystal **1–6** are given in Table 3.

**Synthesis of [LCuCo(NO<sub>3</sub>)<sub>2</sub>] (1), [LCuMn(NO<sub>3</sub>)<sub>2</sub>] (2), <sup>1</sup><sub>∞</sub>[L(H<sub>2</sub>O)CuCo(oxy-bbz)]·CH<sub>3</sub>CN·C<sub>2</sub>H<sub>5</sub>OH (3), [LCuMn(oxy-bbz)(H<sub>2</sub>O)<sub>2</sub>] (4), <sup>1</sup><sub>∞</sub>[L(H<sub>2</sub>O)CuCo(2,5-dhtp)]·CH<sub>3</sub>CN (5) and <sup>1</sup><sub>∞</sub>[L(H<sub>2</sub>O)CuMn(ox)]·3H<sub>2</sub>O (6)**

All starting materials were of reagent grade and were used without further purification. The [LCu] precursor [L<sup>2-</sup> = *N,N'*-propylene-bis-(3-methoxysalicylideneiminato)] was prepared following the procedure published by Pfeiffer *et al.*<sup>14</sup>

**[LCuCo(NO<sub>3</sub>)<sub>2</sub>] (1).** A solution of [LCu] (3 mmol) in acetonitrile:ethanol was reacted with solid Co(NO<sub>3</sub>)<sub>2</sub>·6H<sub>2</sub>O (3 mmol) and stirred for 15 min. Green-blue crystals were obtained upon slow evaporation of the resulted mixture. IR bands (KBr, cm<sup>-1</sup>): 3094 ws, 3065 vw, 2996 vw, 2942 ws, 2927 vw, 2860 ws, 2845 vw, 1613 vi, 1563 w, 1506 m, 1471 i, 1440 i, 1408 m, 1384 m, 1329 m, 1298 vi, 1284 i, 1248 m, 1234 i, 1175 w, 1102 vw, 1070 m, 1026 w, 955 vw, 857 w, 786 w, 746 m, 642 w, 616 w, 572 vw, 538 vw, 471 vw, 444 vw.

**[LCuMn(NO<sub>3</sub>)<sub>2</sub>] (2).** A solution of [LCu] (3 mmol) in acetonitrile:ethanol was reacted with solid Mn(NO<sub>3</sub>)<sub>2</sub>·H<sub>2</sub>O (3 mmol) and stirred for 15 min. Green-brown crystals were obtained upon slow evaporation of the resulted mixture. IR bands (KBr, cm<sup>-1</sup>): 2998 vw, 2950 ws, 2929 w, 2855 vw, 1709 vw, 1614 vi, 1561 m, 1472 vi, 1439 i, 1409 m, 1384 w, 1331 w, 1302 vi, 1234 i, 1174 vw, 1101 vw, 1068 m, 1030 w, 985 vw, 953 vw, 933 vw, 856 w, 816 vw, 786 w, 747 i, 637 vw, 614 vw, 575 vw, 535 vw, 466 vw, 443 vw.

**<sup>1</sup><sub>∞</sub>[L(H<sub>2</sub>O)CuCo(oxy-bbz)]·CH<sub>3</sub>CN·C<sub>2</sub>H<sub>5</sub>OH (3).** A solution of [LCu] (0.02 mmol) in acetonitrile:ethanol was reacted with solid Co(NO<sub>3</sub>)<sub>2</sub> (0.02 mmol). Green-blue crystals of **3** were obtained upon slow diffusion, in a test tube, through an ethanol–water layer (1 mL), of the resulted mixture into an ethanol–water solution of the oxy-bis(benzoic acid) (0.02 mmol) deprotonated by LiOH (0.04 mmol). IR bands (KBr, cm<sup>-1</sup>): 3616 w, 3357 s, 3224 ws, 3091 vw, 2970 vw, 2939 w, 2916 vw, 2837 w, 1618 vi, 1560 i, 1546 i, 1483 m, 1469 i, 1436 w, 1416 w, 1394 w, 1368 i, 1312 i, 1249 i, 1230 i, 1173 w, 1153 w, 1105 w, 1073 m, 1010 w, 988 w, 955 vw, 854 w, 822 w, 789 w, 746 m, 716 m, 658 w, 637 w, 615 vw, 567 vw, 530 vw, 463 vw, 439 vw.

**[LCuMn(oxy-bbz)(H<sub>2</sub>O)<sub>2</sub>] (4).** A solution of [LCu] (0.03 mmol) in acetonitrile:ethanol was reacted with solid Mn(ClO<sub>4</sub>)<sub>2</sub>·6H<sub>2</sub>O (0.03 mmol). Green crystals of **4** were obtained upon slow diffusion, in a test tube, through an ethanol–water layer (1 mL), of the resulted mixture into an ethanol–water solution of the 4,4'-oxybis(benzoic) acid (0.03 mmol) deprotonated by LiOH (0.06 mmol). IR bands (KBr, cm<sup>-1</sup>): 3477 s, 3046 ws, 2976 vw, 2944 vw, 2922 vw, 2874 vw, 2842 vw, 1632 i, 1618 i, 1597 i, 1557 m, 1470 i, 1439 vw, 1373 vi, 1311 m, 1234 vi, 1165 m, 1151 w, 1101 vw, 1069 w, 1012 vw, 980 vw, 953 vw, 935 vw, 878 vw, 856 w, 824 vw, 785 w, 742 m, 703 m, 657 vw, 640 vw, 610 vw, 566 vw, 511 vw, 461 vw, 445 vw.

**<sup>1</sup><sub>∞</sub>[L(H<sub>2</sub>O)CuCo(2,5-dhtp)]·CH<sub>3</sub>CN (5).** A solution of [Cu(valpn)(H<sub>2</sub>O)] (0.02 mmol) in acetonitrile:ethanol was reacted with solid Co(NO<sub>3</sub>)<sub>2</sub> (0.02 mmol). Green-blue crystals of **5** were obtained upon slow diffusion, in a test tube, through an ethanol–water layer (1 mL), of the resulted mixture into an ethanol–water solution of the 2,5-dihydroxy-terephthalic acid (0.02 mmol) deprotonated by LiOH (0.04 mmol). IR bands (KBr, cm<sup>-1</sup>): 3440 s, 3328 vw, 3059 vw, 3014 vw, 2965 vw, 2932 w, 2835 ws, 1621 vi, 1565 w, 1475 i, 1452 i, 1425 i, 1363 w, 1320 m, 1297 i, 1248 vi, 1231 vi, 1104 w, 1075 m, 988 vw, 955 vw, 934 vw, 906 vw, 856 w, 814 w, 785 m, 742 m, 644 w, 614 w, 551 w, 473 vw, 442 vw, 418 vw.

**<sup>1</sup><sub>∞</sub>[L(H<sub>2</sub>O)CuMn(ox)]·3H<sub>2</sub>O (6).** A solution of [LCu] (0.04 mmol) in acetonitrile:ethanol was reacted with solid Mn(NO<sub>3</sub>)<sub>2</sub>·(H<sub>2</sub>O) (0.04 mmol). Green crystals of **6** were obtained upon slow diffusion, in a test tube, through an ethanol–water layer (1 mL), of the resulted mixture into an aqueous solution of the potassium oxalate (0.04 mmol). IR bands (KBr, cm<sup>-1</sup>): 3424 s, 3264 ws, 3060 vw, 2944 ws, 2933 vw, 2921 ws, 2903 ws, 2835 vw, 1634 vi, 1622 vi, 1602 i, 1561 w, 1473 m, 1454 w, 1409 vw, 1369 vw, 1306 m, 1244 m, 1228 i, 1170 vw, 1101 vw, 1073 w, 1006 vw, 987 vw, 955 vw, 856 w, 779 w, 740 m, 637 vw, 613 vw, 565 vw, 508 vw, 469 vw, 438 vw.

## Acknowledgements

Financial support from CNCSIS (grant IDEI 1912/2009) is gratefully acknowledged.

## References

- (a) R. W. Gable, B. F. Hoskins and R. Robson, *J. Chem. Soc., Chem. Commun.*, 1990, 1677; (b) B. F. Hoskins and R. Robson, *J. Am. Chem. Soc.*, 1990, **112**, 1546.
- (a) R. Robson, *J. Chem. Soc., Dalton Trans.*, 2000, 3735; (b) N. R. Champness, *Dalton Trans.*, 2006, 877; (c) B. Moulton and M. J. Zaworotko, *Chem. Rev.*, 2001, **101**, 1629; (d) M. Eddaoudi, D. B. Moler, H. Li, B. Chen, T. M. Reineke, M. O'Keeffe and O. M. Yaghi, *Acc. Chem. Res.*, 2001, **34**, 319; (e) S. Kitagawa, R. Kitaura and S. Noro, *Angew. Chem., Int. Ed.*, 2004, **43**, 2334; (f) C. J. Kepert, *Chem. Commun.*, 2006, 695; (g) S. Kitagawa, S. Noro and T. Nakamura, *Chem. Commun.*, 2006, 701; (h) O. R. Evans and W. Lin, *Acc. Chem. Res.*, 2002, **35**, 511; (i) E. Coronado and J.-R. Galán-Mascarós, *J. Mater. Chem.*, 2005, **15**, 66; (j) D. Bradshaw, J. B. Claridge, E. J. Cussen, T. J. Prior and M. J. Rosseinsky, *Acc. Chem. Res.*, 2005, **38**, 273; (k) S. Kitagawa and S. Noro, in *Comprehensive Coordination Chemistry II*, ed. J. A. McCleverty and T. J. Meyer, Elsevier, Amsterdam, 2004, vol. 7, p. 231.
- (a) H. W. Roesky and M. Andruh, *Coord. Chem. Rev.*, 2003, **236**, 91; (b) G. Janiak, *J. Chem. Soc., Dalton Trans.*, 2000, 3885; (c) H. Schmidbaur, *Chem. Soc. Rev.*, 1995, **24**, 391; (d) A. M. Madalan, N. Avarvari and M. Andruh, *Cryst. Growth Des.*, 2006, **6**, 1671 and references therein; (e) A. N. Khlobystov, A. J. Blake, N. R. Champness, D. A. Lemenovskii, A. G. Majouga, N. V. Zyk and M. Schröder, *Coord. Chem. Rev.*, 2001, **222**, 155; (f) J. K. Katz, K. Sakai and D. B. Leznoff, *Chem. Soc. Rev.*, 2008, **37**, 1884; (g) A. M. Madalan, V. Ch. Kravtsov, Yu. A. Somoov, V. Voronkova, L. L. Korobchenko, N. Avarvari and M. Andruh, *Cryst. Growth Des.*, 2005, **5**, 45; (h) C. Paraschiv, M. Andruh, S. Ferlay, M. W. Hosseini, N. Kyritsakas, J.-M. Planeix and N. Stanica, *Dalton Trans.*, 2005, 1195.
- (a) F. A. Cotton, C. Lin and C. A. Murillo, *Acc. Chem. Res.*, 2001, **34**, 759; (b) M. Andruh, *Pure Appl. Chem.*, 2005, **77**, 1685;



- (c) M. Andruh, *Chem. Commun.*, 2007, 2565 and references therein; (d) M. Andruh, D. G. Branzea, R. Gheorghe and A. M. Madalan, *CrystEngComm*, 2009, **11**, 2571; (e) M. Pascu, M. Andruh, A. Müller and M. Schmidtman, *Polyhedron*, 2004, **23**, 673.
- 5 (a) R. Gheorghe, P. Cucos, M. Andruh, J.-P. Costes, B. Donnadieu and S. Shova, *Chem.-Eur. J.*, 2006, **12**, 187; (b) R. Gheorghe, M. Andruh, A. Müller and M. Schmidtman, *Inorg. Chem.*, 2002, **41**, 5314.
  - 6 J.-P. Costes, F. Dahan, A. Dupuis and J.-P. Laurent, *Inorg. Chem.*, 1996, **35**, 2400.
  - 7 (a) J.-P. Costes, R. Gheorghe, F. Dahan, M. Andruh, S. Shova and J.-M. Clemente Juan, *New J. Chem.*, 2006, **30**, 572; (b) D. G. Branzea, A. Guerri, O. Fabelo, C. Ruiz-Pérez, L.-M. Chamoreau, C. Sangregorio, A. Caneschi and M. Andruh, *Cryst. Growth Des.*, 2008, **8**, 941; (c) D. G. Branzea, L. Sorace, C. Maxim, A. Caneschi and M. Andruh, *Inorg. Chem.*, 2008, **47**, 6590.
  - 8 O. Y. Ma, Z. Han and Y. He, *Chem. Commun.*, 2007, 4107.
  - 9 B. J. Hathaway, in *Comprehensive Coordination Chemistry*, ed. G. Wilkinson, R. D. Gillard and J. A. McCleverty, Pergamon, Oxford, 1987, vol. 5, p. 607.
  - 10 A. B. P. Lever, *Inorganic Electronic Spectroscopy*, Elsevier, Amsterdam, 1984.
  - 11 See, for example: (a) G. De Munno, R. Ruiz, F. Lloret, J. Faus, R. Sessoli and M. Julve, *Inorg. Chem.*, 1995, **34**, 408 and references therein; (b) J. Y. Lu, M. A. Lawandy, J. Li, T. Yuen and C. L. Lin, *Inorg. Chem.*, 1999, **38**, 2698; (c) O. Castillo, A. Luque, J. Sertucha, P. Román and F. Lloret, *Inorg. Chem.*, 2000, **39**, 6142; (d) M. Andruh, R. Melanson, C. V. Stager and F. D. Rochon, *Inorg. Chim. Acta*, 1996, **251**, 309; (e) F. D. Rochon, R. Melanson and M. Andruh, *Inorg. Chem.*, 1996, **35**, 6086; (f) M. C. Muñoz, M. Julve, F. Lloret, J. Faus and M. Andruh, *J. Chem. Soc., Dalton Trans.*, 1998, 3125; (g) R. Lescouëzec, G. Marinescu, M. C. Muñoz, D. Luneau, M. Andruh, F. Lloret, J. Faus, M. Julve, J. A. Mata, R. Llusar and J. Cano, *New J. Chem.*, 2001, **25**, 1224; (h) G. Marinescu, M. Andruh, R. Lescouëzec, M. C. Muñoz, J. Cano, F. Lloret and M. Julve, *New J. Chem.*, 2000, **24**, 527; (i) S. Decurtins, H. W. Schmalle, H. R. Oswald, A. Linden, J. Ensling, P. Gütlich and A. Hauser, *Inorg. Chim. Acta*, 1994, **216**, 65; (j) S. Decurtins, H. W. Schmalle, P. Schneuwly, J. Ensling and P. Gütlich, *J. Am. Chem. Soc.*, 1994, **116**, 9521; (k) Costisor, K. Mereiter, M. Julve, F. Lloret, Y. Journaux, W. Linert and M. Andruh, *Inorg. Chim. Acta*, 2001, **324**, 352.
  - 12 (a) S. Neogi and P. K. Bhardway, *Inorg. Chem.*, 2005, **44**, 816; (b) X.-L. Zhang, B.-H. Ye and X.-M. Chen, *Cryst. Growth Des.*, 2005, **5**, 1609; (c) K. L. Huang, X. Liu, X. Chen and D.-Q. Wang, *Cryst. Growth Des.*, 2009, **9**, 1646.
  - 13 O. Kahn, *Molecular Magnetism*, VCH, New York, 1993, p. 258.
  - 14 P. Pfeiffer, E. Breityh, E. Lülle and T. Tsumaki, *Justus Liebigs Ann. Chem.*, 1933, **503**, 84.